REPORT DOCUMENTATION PAGE

Form Approved
OMB No. 0704-0188

1. AGENCY USE ONLY (Leave Blank)	2. REPORT DATE	3. REPORT TYPE AND DATES COVERED
	25 June 1999	Technical 6/1/98-5/31/99

4. TITLE AND SUBTITLE
Vibrational Sum Frequency Spectroscopy at Liquid-Liquid Interfaces: Model Model Membrane Systems

5. FUNDING NUMBERS
N00014-89-J-1261

6. AUTHOR(S)
Robert A. Walker, Beth L. Smiley, and G. L. Richmond

7. PERFORMING ORGANIZATION NAME(S) AND ADDRESS(ES)

Dept. of Chemistry
University of Oregon
Eugene, OR 97403

8. PERFORMING ORGANIZATION REPORT NUMBER

ONR Technical Report #29

9. SPONSORING/MONITORING AGENCY NAME(S) AND ADDRESS(ES)

Dr. Peter Schmidt
Office of Naval Research Physical Science and Technology, ONR 331
800 North Quincy Street
Arlington, VA 22217-5000

10. SPONSORING/MONITORING AGENCY

Office of Naval Research

11. SUPPLEMENTARY NOTES

Spectroscopy, submitted May 1999

12A. DISTRIBUTION / AVAILABILITY STATEMENT

Approved for public release: distribution unlimited

12B. DISTRIBUTION CODE

13. ABSTRACT (Maximum 200 words)

Please see attached abstract

14. SUBJECT TERMS
Vibrational Sum Frequency Generation (VSFG) characterization of liquid:liquid interfaces

15. NUMBER OF PAGES
32

16. PRICE CODE

17. SECURITY CLASSIFICATION OF REPORT	18. SECURITY CLASSIFICATION OF THIS PAGE	19. SECURITY CLASSIFICATION OF ABSTRACT	20. LIMITATION OF ABSTRACT
Unclassified	Unclassified	Unclassified	

OFFICE OF NAVAL RESEARCH

Grant N00014-89-J-1261

R&T Code 4131038

ONR Technical Report ONR Technical Report #29

Vibrational Sum Frequency Spectroscopy at Liquid-Liquid Interfaces: Model Model Membrane Systems

by

Robert A. Walker, Beth L. Smiley, and G. L. Richmond

Spectroscopy, submitted May 1999

Department of Chemistry
1253 University of Oregon
Eugene, OR 97403

June 1999

Submitted to Spectroscopy

Vibrational Sum Frequency Spectroscopy at Liquid—Liquid Interfaces: Model Membrane Systems

Robert A. Walker[a], Beth L. Smiley, and Geraldine L. Richmond*

Department of Chemistry, University of Oregon, Eugene, OR 97403

Abstract: Vibrational sum frequency spectroscopy (VSFS) has evolved into a versatile technique for assessing molecular structure of complex systems adsorbed to condensed phase interfaces. One field of research particularly well suited to the strengths of VSFS is biological interfaces. Traditionally, structural characterization of biologically important surfaces has proven difficult at the molecular level of detail. However, VSFS can determine the conformation and orientation of specific functional groups belonging to adsorbed species. This paper discusses issues pertinent to VSFS experiments at liquid:liquid interfaces and shows how this technique can be applied to study the structure of model membrane systems.

I. Introduction

Examples of interfaces in biology range from membrane surfaces to capillaries to retinae to the air:tissue boundary in lung alveoli. [1-4] Given the crucial role which interfaces play in a wide variety of biological processes, a need has arisen for experimental techniques capable of examining molecularly and interfacially specific properties of biological systems. Molecular specificity refers to the ability of an experiment to directly determine the orientation and conformation of specific molecular functional groups. Interfacial specificity requires that an experiment be capable of discriminating a response of molecules at an interface from responses arising in either bulk medium. During the past decade second order nonlinear optical spectroscopy has emerged as a powerful, *in situ* technique which satisfies these demanding criteria. [5-7] In particular, vibrational sum frequency spectroscopy (VSFS) provides a means by which one can aquire vibrational spectra of molecules at interfaces. [8-10] In this article we consider a number of issues essential for carrying out VSFS experiments at a liquid:liquid interface and show how this method can be applied to examine model biological systems adsorbed at this boundary.

Conceptually, VSFS is a simple technique: two coherent optical fields overlap both spatially and temporally at the interface being studied. (Figure 1) One of these fields is of fixed frequency in the visible region (ω_{vis}) while the other is tunable in the infrared (ω_{ir}). Whenever ω_{ir} is resonant with an allowed vibrational transition of a molecule in the interfacial region, the two fields couple through a resonant piece of the second order nonlinear susceptibility, $\chi^{(2)}$, to produce a third field equal in energy to the sum of $\omega_{ir} + \omega_{vis} = \omega_{sum}$. Scanning ω_{ir} and monitoring intensity at ω_{sum} leads to a vibrational spectrum of molecules in interfacial environments. Researchers first used VSFS to examine the structure of Langmuir monolayers adsorbed to vacuum:solid, [11] air:solid[12] and air:liquid[13] surfaces. Subsequent studies extended this technique to buried interfaces or interfaces between two condensed phases. [8, 14] Liquid:liquid interfaces are particularly

important in the study of biological systems since they provide a realistic model of environments commonly found *in vivo*. [3]

Recently, we have used VSFS to study the structure of phosphatidylcholine (PC) monolayers adsorbed to an aqueous:CCl_4 interface. [15-19] Although this interface is distinctly "non-biological", it does mimic the aqueous:hydrophobic junction found in many biological systems including membranes. [20] Phosphatidylcholines are amphiphilic molecules possessing two long acyl chains connected to a zwitterionic headgroup by means of a three carbon glycero backbone. (Figure 2) These phospholipids are a major component of most cell membranes and, consequently, have been the subject of intense scientific scrutiny over the past three decades. Cell membranes generally consist of a lipid bilayer structure, and PC monolayers have served as simple model membranes. [21, 22] Surface tension[23, 24] and fluorescence microscopy [25-27] experiments have attempted to correlate monolayer composition with properties such as permeability, compressibility and thermodynamic phase. These studies revealed rich thermodynamic phase behavior in these monolayers as well as structural transitions on length scales of microns. A limiting aspect of these results, however, is their inability to provide information about the *microscopic* structure of the adsorbed monolayers.

Employing VSFS to study PC monolayers can answer specific questions about molecular conformation and monolayer ordering at interfaces. From vibrational spectra of PC monolayers adsorbed at a liquid:liquid interface, we ascertain how molecular structure of the monolayer depends on variables such as acyl chain length, surface concentration, temperature and, by inference, the degree of chain solvation by the organic solvent. [15] VSFS experiments have also uncovered important aspects about the structure of water molecules in the vicinity of PC monolayers[16] - information which should prove helpful to theorists seeking to model membranes by molecular dynamics simulations. [28-30] The union of VSFS results with simulation data promises to provide a comprehensive, detailed understanding of these model membrane systems.

The next two sections of this article address the origin of the sum frequency response from an interface and a number of experimental considerations pertinent to nonlinear spectroscopic experiments at buried interfaces. Following the experimental considerations are examples of how VSFS has been applied to studies of PC monolayer structure at an aqueous:CCl_4 interface. This section details how different preparation methods can give rise to monolayers having remarkably different structural characteristics. Vibrational band positions and intensities in a vibrational sum frequency (VSF) spectrum coupled with VSFS selection rules can be used to determine the degree of ordering found within monolayers. VSF spectra also elucidate the structure of solvating water molecules in the interfacial region. These studies of solvent structure further emphasize the power of VSFS to paint a complete picture of molecular structure at interfaces. We conclude with some thoughts on the future application of VSFS to more complicated biological systems.

II. Origin of the nonlinear sum frequency signal

When an oscillating electric field interacts with a molecule, the field induces a time-dependent oscillating dipole. In condensed phases, this microscopic effect manifests itself as a macroscopic induced polarization, P, which can be expanded in a Taylor series:

$$P = P^{(0)} + P^{(1)} + P^{(2)} + \ldots \quad (1)$$

Typically, the induced polarization depends linearly on the strength of the impinging field and the expansion may be truncated after the first order term, $P^{(1)}$. However, in the presence of sufficiently strong fields (such as those produced by lasers), higher order terms must be included to accurately characterize the induced polarization. The second order polarizability, $P^{(2)}$, gives rise to sum frequency generation and is expressed as a product of the incident electric field(s) and second order, nonlinear susceptibility tensor, $\chi^{(2)}$,

$$P^{(2)} = \chi^{(2)} : E_1(t)E_2(t) \quad (2)$$

In a typical VSF experiment, E_1 and E_2 represent the fixed frequency visible (ω_{vis}) and tunable infrared (ω_{ir}) fields, respectively. The intensity of the sum frequency response is proportional to the square of the induced second order polarization:

$$I(\omega_{sum}) \propto \left|P^{(2)}\right|^2 \propto \left|\chi^{(2)}\right|^2 I(\omega_{vis}) I(\omega_{ir}) \tag{3}$$

where $I(\omega_{vis})$ and $I(\omega_{ir})$ correspond the intensities of the visible and infrared fields.

Interfacial specificity in VSFS arises from the symmetry properties of $\chi^{(2)}$. Since $\chi^{(2)}$ is a third rank tensor, it necessarily changes sign upon inversion ($\chi^{(2)}_{ijk} = -\chi^{(2)}_{-i-j-k}$). Within the electric dipole approximation, this condition forbids sum frequency generation in isotropic media. At interfaces, however, the inversion symmetry found in such media is necessarily broken and the sum frequency generation becomes symmetry allowed.

Contained within the $\chi^{(2)}$ tensor are twenty seven elements which completely characterize the nonlinear susceptibility for all combinations of incident and sum frequency polarizations. Imposing $C_{\infty v}$ symmetry about the interfacial normal reduces the number of nonzero $\chi^{(2)}$ elements to four: $\chi^{(2)}_{zzz}$, $\chi^{(2)}_{zii}$, $\chi^{(2)}_{izi}$, $\chi^{(2)}_{iiz}$, where subscripts refer to the directional nonlinear susceptibility for the sum frequency, visible and infrared fields, respectively [31]. In the lab fixed frame i = x or y and z lies normal to the interface. When far from electronic resonances, Kleinman symmetry renders $\chi^{(2)}_{zii}$ and $\chi^{(2)}_{izi}$ equivalent. Selecting different polarizations of the infrared, visible and reflected sum frequency fields samples different subsets of these $\chi^{(2)}$ elements:

$$I_{ppp} \propto \left|\tilde{f}_z f_z f_z \chi^{(2)}_{zzz} + \tilde{f}_z f_i f_i \chi^{(2)}_{zii} + \tilde{f}_i f_z f_i \chi^{(2)}_{izi} + \tilde{f}_i f_i f_z \chi^{(2)}_{iiz}\right|^2 \tag{4a}$$

$$I_{ssp} \propto \left|\tilde{f}_i f_i f_z \chi^{(2)}_{iiz}\right|^2 \tag{4b}$$

$$I_{sps} \propto \left|\tilde{f}_i f_z f_i \chi^{(2)}_{izi}\right|^2 \tag{4c}$$

The subscripts on the sum frequency intensity refer to the polarization of the sum frequency, visible and infrared fields with respect to the surface plane in order of descending frequency. The factors $\tilde{f}_{i,Z}$ and $f_{i,z}$ represent the nonlinear and linear Fresnel factors governing the transmittance and reflectance of electromagnetic fields at interfaces.

Each individual $\chi^{(2)}$ element may be further broken down into a nonresonant and resonant component: [32]

$$\chi^{(2)}_{ijk} = \chi^{(2)}_{ijk,nr} + \sum_{\upsilon} \chi^{(2)}_{ijk,\upsilon} \tag{5}$$

The non-resonant piece, $\chi^{(2)}_{ijk,nr}$, is characteristic of the materials on either side of the interface while the resonant contribution, $\chi^{(2)}_{ijk,\upsilon}$, is summed over all contributing vibrations of molecules in the interfacial region. For nonconducting systems, $\chi^{(2)}_{ijk,nr}$ is quite small relative to the resonant sum over vibrational states. Through the molecular hyperpolarizability, β, the resonant component of a $\chi^{(2)}$ element can be related to a particular vibration's infrared and Raman activity:

$$\chi^{(2)}_{ijk,\upsilon} = \frac{N}{\varepsilon_0} \langle \beta_\upsilon \rangle \tag{6}$$

where

$$\beta_\upsilon = \frac{A_\upsilon M_{\upsilon,g}}{\omega_{ir} - \omega_0 - i\Gamma} \tag{7}$$

The factor of N in Equation 6 represents the number of sampled molecules and the brackets on β imply an orientationally averaged distribution. The numerator of Equation 7 contains the infrared (A_υ) and Raman ($M_{\upsilon,g}$) transition matrix elements. Molecules in the interfacial region can not possess inversion symmetry otherwise the numerator in this expression will vanish by mutual exclusion. The denominator predicts a strong resonant enhancement in the observed sum frequency intensity whenever ω_{ir} approaches ω_0, the frequency of an allowed vibrational transition.

III. Experimental considerations

A. Optical requirements

The most challenging technical aspect of VSFS involves generation of tunable infrared radiation with sufficient intensity. Possible sources include a number of optical parametric processes (generation, oscillation, amplification) [33, 34] as well as difference frequency mixing[35] and stimulated Raman scattering. [8] In our laboratory we have employed several different optical systems to carry out VSFS experiments at liquid:liquid interfaces. Two of these systems are built around nanosecond Nd:YAG lasers while a third relies on a picosecond Ti:Sapphire regeneretivly amplified apparatus. The characteristics of all three systems are summarized in Table 1.

System 1 consists of an extended cavity Nd:YAG (GCR-11, Spectra Physics) which produces ~200 mJ at 1064 nm with a repetition rate of 10 Hz and a pulse duration of 13 ns. [34] A fraction of the 1064 nm output is frequency doubled in a KTP crystal and used as ω_{vis}. The remaining 1064 pumps a home built $LiNbO_3$ optical parametric oscillator which provides tunable infrared radiation from 3.0 - 3.6 μm (3300 - 2800 cm^{-1}). With a spectral bandwidth of only 6 cm^{-1}, this system resolves most vibrational bands in theVSF spectra described in this work.

The optical equipment of System 2 includes a Ti:Sapphire oscillator (Mira900, Coherent) which seeds a Nd:YLF pumped Ti:Sapphire regenerative amplifier (Quantronix) to produce 0.8 W of 800 nm radiation. [33] VSFS experiments carried out with System 2 used ~650 μJ of the 800 nm output to pump an ethylene glycol white light generation/KTP optical parametric amplifier assembly which produces tunable infrared radiation over a wide window, 2.7 - 4.0 μm (3700 - 2500 cm^{-1}). Experiments carried out with System 2 are up to 10^3 times more sensitive than experiments conducted with System 1 due to differences in pulse duration (2 picoseconds for System 2, 13 nanoseconds for System 1). Equation 3 shows that the sum frequency signal depends upon the peak intensities of both the incident visible and infrared fields. With pulse durations of only 2 ps, the instantaneous peak

powers of System 2 are 50 - 100 times higher than those of System 1. A repetition rate of 1 kHz allows greater signal averaging and further improvements in signal to noise over System 1. The major drawback to System 2 is its spectral resolution of 16 cm^{-1}. This bandwidth is not always able to resolve adjacent features in a VSF spectrum.

Recently, we have completed construction of a third optical system for VSFS studies of buried interfaces. System 3 relies upon the 1064 nm output of an injection seeded Nd:YAG (Infinity, Coherent) to pump a commercial KTP optical paremetric oscillator/optical parametric amplifier assembly (LaserVision). Currently this system produces tunable infrared radiation from 2.5 μm (4000 cm^{-1}) to 4.2 μm (2400 cm^{-1}), although this can be extended deeper into the infrared using other crystals. The pulse duration of the infrared pulses is ~3.5 ns making this system 10 times more sensitive than System 1. Other attractive aspects include improved resolution (2 cm^{-1} bandwidth) and a variable repetition rate (1 - 100 Hz) to aid in signal averaging.

B. Geometry

All VSF spectra of monolayers adsorbed to a liquid:liquid interface were acquired in a total internal reflection (TIR) geometry. [14, 34] Experimentally, this condition requires that ω_{vis} and ω_{ir} approach the interface through the high index medium (CCl_4) and that the sum frequency signal (ω_{sum}) departs from the interface at its critical angle. This configuration endows the experimental arrangement with remarkably enhanced sensitivity. This improved sensitivity results from the behavior of the Fresnel factors under conditions of total internal reflection. Bloembergen and Pershan first prediced that a TIR geometry would amplify second order nonlinear optical processes at interfaces. [36] Two decades later a number of independent experiments demonstrated this effect at air:solid [37] and liquid:liquid[38] interfaces. Examination of Eq. 4a - 4c shows that the intensity of the detected sum frequency signal depends on the square of the nonlinear susceptibility and the

square of the product of the appropriate Fresnel factors. The linear (f_i) and nonlinear ($\tilde{f}_i$) Fresnel factors have the following form: [37]

$$f_i = \frac{2\sin\theta_u}{\sin(\theta_i+\theta_u)} \begin{pmatrix} \cos\theta_u / \cos(\theta_u - \theta_i) \\ \cos\theta_i \\ \left(\frac{n_i}{n_u}\right)\cos\theta_u / \cos(\theta_u - \theta_i) \end{pmatrix} \tag{7a}$$

$$\tilde{f}_i = a\frac{\sin\theta_t}{\sin(\theta_r+\theta_t)} \begin{pmatrix} -\cos\theta_t / \cos(\theta_t - \theta_r) \\ 1 \\ \left(\frac{n_t}{n_m}\right)^2 \sin\theta_r / \cos(\theta_t - \theta_r) \end{pmatrix} \tag{7b}$$

The angles θ_u and θ_i are the angles of incidence and refraction for the incident visible and infrared fields with respect to the surface normal, while n_i and n_u are the refractive indices for CCl_4 and water. In Equation 7b, θ_t and θ_r represent the angles of sum frequency transmission and reflection respectively. The refractive index for water appears as n_t, and n_m represents the refractive index of the interfacial region, assumed to be intermediate between the indices of water and CCl_4. The coefficient *a* contains a number of optical constants as defined in Reference 37. Figure 3 plots $\left|\tilde{f}_i f_i f_z\right|^2$ as a function of incident angle for conditions of internal and external reflection. (External reflection refers to a geometry in which optical fields pass through the medium having the lower refractive index.) Near 68° the square of the Fresnel factor product for internal reflection exhibits sharply peaked, $>10^2$ fold enhancement over the same quantity for external reflection conditions. From a practical standpoint, this condition requires that ω_{vis} approach the interface at its critical angle (65.8°) and the angle of ω_{ir} be adjusted to maximize the sum frequency signal.

IV. Results

A. Polarization dependent studies of chain orientation

Given their amphiphilic structure, PCs adsorb to a liquid:liquid interface with the zwitterionic headgroup solvated in the aqueous phase and the acyl chains dissolving in the CCl_4. Different aspects about the structure of the same PC monolayer can appear in VSF spectra acquired under different polarization conditions. Figure 4 displays spectra of a dilauroylphosphatidylcholine (DLPC, C_{12}) monolayer acquired under different polarization conditions using System 1. Surface tension measurements indicated that the DLPC monolayer had a surface coverage of 1.8×10^{14} molecules/cm^2. The spectra contain different combinations of vibrational bands, a condition which reflects the different subsets of nonzero $\chi^{(2)}$ elements sampled by the various polarization conditions (Equations 4 a-c). Interpreting the features in the CH stretching region of a VSF spectrum can prove challenging due to the number of potential contributing oscillators. Nevertheless, infrared, Raman and deuteration data [39, 40] enable us to make assignments of individual VSF bands and draw conclusions about monolayer orientation at an aqueous:CCl_4 interface.

A spectrum taken under $P_{sum}P_{vis}P_{ir}$ (or PPP) conditions appears in the top panel and contains a large number of vibrational bands. This spectral complexity arises from the contribution of multiple $\chi^{(2)}$ elements as predicted by Equation 4a. These bands include the symmetric stretches of acyl methylene and methyl groups (d^+ and r^+) at 2850 cm^{-1} and 2872 cm^{-1}, the methyl asymmetric stretch (r^-) at ~2965 cm^{-1}, and a broad Fermi resonance interaction centered at 2900 cm^{-1} arising from overtones of methylene bending motion (CH_2 FR). The largest feature in the PPP spectrum appears at 2935 cm^{-1} and probably contains contributions from the methylene asymmetric stretch (d^-) and a methyl Fermi resonance (CH_3 FR). [13, 34] The high energy shoulder on r^- is assigned to the symmetric stretch of methyl groups attached to the quarternary ammonium on the headgroup. [41]

In an SSP spectrum (middle panel) only a single $\chi^{(2)}$ element contributes to the observed spectral intensity (Equation 4b). Consequently, an SSP spectrum is considerably simpler than a spectrum acquired under PPP conditions. Intensity in an SSP spectrum arises from vibrational motion normal to the interface and three features dominate the CH

stretching region: d^+, r^+, and the d^-/CH_3 FR band. Conspicuous in its absence is r^-. The combination of a strong r^+ band and absent r^- band implies that the methyl groups of the acyl chains have their C_3 axes aligned, on average, normal to the interface.

Supporting this claim is the SPS spectrum in the bottom panel of Figure 4. The SPS polarization condition again samples a single $\chi^{(2)}$ element which is sensitive to vibrational motion in the plane of the interface. In the SPS spectrum r^- stands out as the largest feature, r^+ is absent and d^+ appears very weakly. The broad, unresolved intensity between 2880 and 2940 cm^{-1} may contain contributions from CH stretching motion along the glycero backbone.[42] With the acyl methyl groups aligned normal to the interface, we expect that infrared transition dipole of r^- to lie in the plane of the interface while r^+ has its infrared transition dipole aligned normal to the interface. The presence/absence of these features in the SSP and SPS spectra implies that the acyl methyl groups in the DLPC monolayer assume a rotationally isotropic distribution. These observations support the assumption of interfacial $C_{\infty v}$ symmetry made when reducing the $\chi^{(2)}$ tensor in Section II.

B. Monolayer ordering as a function of preparation method

Order within a PC monolayer can be characterized by two limiting cases. In an ordered monolayer acyl chains assume primarily all-*trans* conformations and their chain axis aligns normal to the interface (upper panel, Figure 4). A disordered monolayer is one in which acyl chains possess either *gauche* defects or simple torsional distortion along the carbon backbone (lower panel, Figure 4). The differences between ordered and disordered monolayers manifest themselves quite clearly in VSF spectra.

As a consequence of the extended symmetry found in all-*trans* hydrocarbon chains, the infrared active methylene symmetric stretch ($d^+(0)$) is 180° out of phase with the Raman active methylene symmetric stretch ($d^+(\Pi)$). [40] This condition leads to a vanishing numerator in Eq. 7. In other words, d^+ is sum frequency forbidden in the all-*trans* acyl chains which make up an ordered PC monolayer. Conformational disorder lifts the

symmetry constraints imposed on the methylene symmetric stretch, [39] and in disordered chains d^+ becomes sum frequency allowed. No such symmetry restrictions apply to the methyl symmetric stretch (r^+); r^+ is never sum frequency forbidden by symmetry in a monolayer. *Consequently, a ratio comparing the integrated intensities of r^+ and d^+ can be used to gauge the degree of disorder found within the acyl chains making up a monolayer.* In the limit of a highly ordered monolayer, the r^+/d^+ ratio becomes quite large with methyl groups all aligned normal to the interface and VSF inactive methylene vibrations. As a monolayer becomes disordered, methylene units begin to contribute to the d^+ band, and the r^+/d^+ ratio becomes smaller. We use r^+/d^+ ratios from SSP spectra to analyze monolayer ordering given this polarization condition's sensitivity to vibrational motion normal to the interface. [15, 17]

Phosphatidylcholine monolayers adsorbed to the aqueous:CCl_4 interface can be prepared by a number of different methods. The three ways in which we prepare monolayers are a) from decomposition of PC vesicles; b) from multiple injections of aqueous PC dispersions; and c) from a newly developed spreading technique. [43] Results presented below will demonstrate that these preparation procedures can lead to different degrees of interfacial ordering within PC monolayers.

Formation of monolayers from the decomposition of vesicles (DV monolayers) relies upon the tendency of PC vesicles to break apart at interfaces to form monolayers of PC monomers. [44] An important aspect of DV monolayers is that these monolayers form in accordance with the equilibrium established between PC vesicles in solution and the PC monomers adsorbed at the interface. [19] Surface coverage is not independently variable. Rather, coverage depends on temperatue and bulk PC concentration.

Both the multiple injection and spreading solvent methods afford a degree of external control over monolayer surface concentration in contrast to the vesicle decomposition technique. The multiple injection technique involves making repeated injections of an aqueous PC suspension into the aqueous phase overlaying the CCl_4 phase.

[18] This procedure leads to the formation of tightly packed monolayers (MI monolayers) as evidenced by high surface pressures (42 mN/m) and a reduction in the interfacial meniscus. Recently, we have begun preparing monolayers at the aqueous:CCl_4 interface by using PCs dissolved in a chloroform spreading solvent (SS monolayers). After dissolving the desired PC in the chlorofom, we use a microsyringe to deposit small droplets of the PC/chloroform solution at the liquid:liquid interface. Surface tension keeps the droplets at the interface before the droplets dissolve into the CCl_4 subphase, long enough for the amphiphilic PC monomers to spread and form a monolayer. Surface pressure and VSFS data from SS monolayers mimic results acquired from comparable MI monolayers.

Evidence that the choice of preparation method affects PC monolayer structure comes from comparing the r^+/d^+ ratio of DV monolayers with the ratio found for MI and SS monolayers. Figure 5 displays VSF spectra (SSP) of distearoylphosphatidylcholine (DSPC, C_{18}) monolayers prepared by the vesicle decomposition (top panel) and multiple injection (middle panel) techniques. For comparison Figure 5 contains a VSF spectrum of a DSPC monolayer at the air:water interface (bottom panel). Spectra of the DV and MI monolayers were recorded with System 1; the VSF spectrum of the DSPC monolayer at the air:water interface was recorded with System 3. All three spectra contain the same features: d^+ at 2850 cm^{-1}, r^+ at 2872 cm^{-1}, and a band at 2925-2940 cm^{-1} which contains contributions from the methylene asymmetric stretch (d^-) and a methyl Fermi resonance interaction (CH_3 FR). Although the surface coverages of the DV and MI monolayers are approximately equal (as evidenced by similar surface pressures), the DV monolayer exhibits appreciable disorder (r^+/d^+ ratio of 0.5) while the MI monolayer shows a high degree of acyl chain ordering ($r^+/d^+ = 5.3$). Monolayers of DSPC at the aqueous:CCl_4 interface prepared from a spreading solvent also show very large r^+/d^+ ratios. (Spectrum not shown.)

The contrast in conformational order between the DV and MI monolayers seems somewhat surprising. Surface tension studies indicate that DSPC DV monolayers have terminal surface concentrations of 1.8×10^{14} molecules/cm^2 or, equivalently, molecular areas of 55 A^2/molecule. This coverage lies close to the limiting surface coverage of 2.1×10^{14} molecules/cm^2 (48 Å^2/molecule) reported in Langmuir trough experiments carried out on PC monolayers at alkane:water interfaces. [23, 24] Hard sphere models show the PC headgroup to have a cross sectional area of 45 Å^2 (along the long axis) while a pair of all-*trans* acyl chains occupy 42 Å^2. [45] If the second injection in the multiple injection technique compresses the existing incomplete MI monolayer *and* the limiting surface PC coverage at the aqueous:CCl_4 interface agrees with results from alternative aqueous:organic interfaces, then the MI monolayer could conceivably have a *slightly* higher (by no more than 15%) surface concentration than that of the DV monolayer. This subtle change in surface coverage, however, appears to cause dramatic structural changes in the monolayer.

We have interpreted the disorder found in the DSPC DV monolayer as evidence of acyl chain solvation by the CCl_4 solvent. The presence of solvent molecules within the acyl chain network will screen attractive chain-chain van der Waals interactions and result in a more disordered monolayer. An injection induced compression may expel solvent molecules from between the hydrocarbon chains and induce a transition to a two dimensional liquid crystalline state of the monolayer. Expulsion of solvent would explain the similarities observed between the DSPC-MI monolayer and the DSPC monolayer at the air:water interface.

More extensive studies on the effect of chain length on conformational order support the idea that chain solvation plays an important role in deteriming monolayer structure. Figure 6 contains the r^+/d^+ ratios calculated from spectra of monolayers formed from the DV, MI and SS methods as a function of chain length. Also included for comparison are the ratios of monolayers at the air:water interface. For PC species with

chain lengths $\leq C_{16}$, MI and SS monolayers show a similar degree of order to that of DV monolayers. However, acyl chain order increases dramatically in the longer chain species (C_{17} - C_{20}) when monolayers are formed by spreading solvent or multiple injections. From these observations we infer that monolayers composed of shorter chain species possess a similar degree of permeability to CCl_4 regardless of preparation technique. As PC chain length becomes longer, attractive interchain forces eventually grow strong enough so that small changes in surface concentration can induce a high degree of ordering withing the monolayer. Similarities in the r^+/d^+ behavior between MI/SS monolayers at the aqueous:CCl_4 interface and PC monolayers at the air:water interface strongly suggest a reduced degree of acyl chain solvation in these monolayers at the liquid:liquid interface. Because of the equilibrium responsible for formation of DV monolayers, the surface concentration in these monolayers may never become high enough to expel the CCl_4.

C. Aqueous solvent structure at a liquid:liquid interface

In addition to the insight it sheds on monolayer order and conformation, VSFS is also sensitive to the structure of surrounding solvent molecules. [46] Figure 8 displays the SSP spectrum of a DLPC DV monolayer acquired with System 2. The poorer spectral resolution compared to that of System 1 (16 cm^{-1} vs 6 cm^{-1}) causes the d^+ and r^+ bands overlap. Prominent in the spectrum is a broad symmetric band centered at ~3180 cm^{-1} which we assign to a vibrational mode of water molecules aligned normal to the interface.

Previous VSF studies of water at interfaces[47, 48] have identified three distinguishable OH bands: two bands are broad (~200 cm^{-1} FWHM) and centered at 3200 cm^{-1} and 3400 cm^{-1} while the third band is considerably narrower (~30 cm^{-1} FWHM) and appears at 3680 cm^{-1}. The narrow peak is assigned to the free OH stretch of water molecules missing one hydrogen bond. [47] This feature disappears from VSF spectra whenever an amphiphile - charged or uncharged - adsorbs to the interface. [47, 49, 50] Based on infrared and Raman studies carried out on bulk water, [51-53] the band at

3200 cm^{-1} is assigned to the symmetric stretch of water molecules in symmetrically hydrogen bonded environments (OH SS-S). Lying to higher energies (~3400 cm^{-1}) is the band associated with the symmetric stretch of water molecules in asymmetrically hydrogen bonded environments (OH SS-A). The OH SS-S is the predominant feature found in Raman and infrared studies of bulk ice, while the OH SS-A dominates spectra of liquid water. [51-53]

Intensity in the water region of Figure 8 can be fit to a single OH feature at 3178 cm^{-1} (180 cm^{-1} FWHM) which we assign as the OH SS-S band. Attempts to include a second OH peak (OH SS-A) in the fitting routine show that any feature near 3400 cm^{-1} contributes to no more than 5% of the observed signal. Based on these findings, we conclude that water molecules aligned normal to the interface are highly ordered and experiencing a relatively high degree of ice-like hydrogen bonding. These results agree with earlier studies of water structure at hydrophobic interfaces. [46, 47] Preliminary results from SPS spectra indicate that the solvent environment parallel to the aqueous:CCl_4 interface contains greater disorder with up to 15% of the observed intensity resulting from the OH SS-A band. [16]

VI. Future directions

Applying VSFS to biologically important model systems adsorbed at buried interfaces affords researchers unprecedented opportunity to examine molecular orientation and conformation with molecular specificity. The ability to obtain vibrational spectra of molecules in the interfacial region allows strong connections to be made between molecular structure, macroscopic phenomena, and results from molecular modeling. Results presented in this paper highlight a number of experiments carried out to deduce structural features of PC monolayers adsorbed to an aqueous:CCl_4 interface. From the spectra we have begun to characterize average orientation of the adsorbed amphiphiles, acyl chain ordering within the monolayer, and the structure of surrounding water molecules.

Additional questions regarding the structure of PC headgroups and backbones still remain. We intend to further characterize the molecular structure within PC monolayers by extending the tunability of ω_{ir} to lower frequencies (with different nonlinear optical crystals) and investigate orientation of PC carboxyl and phosphate groups. A logical extension of these PC monolayer studies involves examining the structure of more complicated, heterogeneous monolayers. Model membrane systems frequently consist of a homogeneous, single component monolayer or bilayer. [26] Actual membranes are much more diverse possessing many different types of phospholipids (PCs, phosphoethanolamines, phosphoserines, etc) as well as cholesterol and membrane proteins. [1] With VSFS researchers can potentially answer questions about how different membrane components affect orientation and conformational order within multicomponent monolayers.

With the increasing use of broadband high power infrared and CCD cameras in spectroscopy, [54, 55] VSFS may soon be used to study the kinetics of interfacial processes including monolayer formation. On the timescale of minutes to hours required to form phospholipid monolayers, a 1 kHz laser system used in conjuction with a CCD camera has the potential to record an entire VSF spectrum of the interface every milisecond. Such experiments would take "snapshots" of interfacial vibrational structure at different stages of the monolayer formation process. In this way, researchers could track the evolution of amphiphile and surrounding solvent structure as the monolayer passes from a two dimensional gas phase through different condensed phases on the way to formation of a two dimensional crystalline solid. The feasibility of such experiments has already been demonstrated; we have used System 2 to study interfacial dynamics of DLPC monolayer formation from a solution of DLPC vesicles. [16] Although acquiring spectra in the current experimental configuration requires sweeping ω_{ir} through its tuning range and monitoring ω_{sum} with a photomultiplier tube, the 1kHz repetition rate allows us to acquire a complete

spectrum of the CH and OH stretching region every three minutes. Preliminary findings reveal systematic intensity fluctuations in both the PC and water VSF bands. [16]

Questions about specific molecular interactions can be answered by ultrafast VSFS experiments which probe vibrational relaxation and dephasing. Studies have already used a pump-probe adaptation of VSFS to examine vibrational relaxation of adsorbates on solid surfaces. [11] Extending this technique to systems of biological interest could lead to important insight into a number of phenomena including the mechanism of anaesthetic action and the interaction of metal cations with membrane proteins. These topics have received considerable attention in molecular dynamics simulations and transient absorption experiments. [56, 57] However, empirical data with interfacial specificity remains elusive.

As the field of second order nonlinear optical spectroscopy matures, its techniques are applied to more complicated systems. Due to the molecular and interfacial specificity inherent in these techniques, they have become popular means with which to study a wide variety of interfaces. This paper has discussed using VSFS to study molecular structure of biologically important membrane models adsorbed to a liquid:liquid interface. Receiving particular attention were the issues of the nonlinear sum frequency response and the requirements for carrying out VSFS experiments at buried interfaces. We look forward to deepening our understanding of membrane structure and formation dynamics by means of VSFS and eagerly anticipate new and innovative applications of this powerful technique to additional systems of biological interest.

Acknowledgments

The authors gratefully acknowledge Dr. John Conboy for helpful discussions and Lawrence Scatena for his preliminary investigations of water structure at the neat aqueous:CCl_4 interface. Funding from the Office of Naval Research and the National Science Foundation (CHE-9725751) is deeply appreciated.

Bibliography

[a]current address: Department of Chemistry and Biochemistry, University of Maryland, College Park, MD 20742

[1] M. N. Jones, D. Chapman, *Micelles, Monolayers, and Biomembranes*, Wiley-Liss, New York 1995.

[2] S. A. Safran, *Statistical thermodynamics of surfaces, interfaces and membranes, Vol. 90*, Addison-Wesley Publishing Company, New York 1994.

[3] K. S. Birdi, *Lipid and Biopolymer monolayers at liquid interfaces*, Plenum Press, New York 1989.

[4] V. Volkov, Y. P. Svirko, V. F. Kamalov, L. Song, M. A. El-Sayed, *Biophys. J., 73* (1997) 3164-3170.

[5] Y. R. Shen, *Nature, 337* (1989) 519-525.

[6] K. B. Eisenthal, *Ann. Rev. Phys. Chem., 43* (1992) 627-661.

[7] R. M. Corn, D. A. Higgins, *Chem. Rev., 94* (1994) 107-125.

[8] C. D. Bain, *J. Chem. Soc. Faraday Trans., 91* (1995) 1281-1296.

[9] G. L. Richmond, *Anal. Chem., 69* (1997) 536a-543a.

[10] Y. R. Shen, *Solid State Comm, 102* (1997) 221-229.

[11] A. L. Harris, L. Rothberg, L. H. Dobois, N. J. Levinos, L. Dhar, *Phys. Rev. Lett., 64* (1990) 2086-2089.

[12] N. Akamatsu, K. Domen, C. Hirose, *J. Phys. Chem., 97* (1993) 10070-10075.

[13] P. Guyot-Sionnest, J. H. Hunt, Y. R. Shen, *Phys. Rev. Lett., 59* (1987) 1597-1600.

[14] M. C. Messmer, J. C. Conboy, G. L. Richmond, *J. Am. Chem. Soc., 117* (1995) 8039-8040.

[15] R. A. Walker, J. A. Gruetzmacher, G. L. Richmond, *J. Am. Chem. Soc., in press* (1998) .

[16] R. A. Walker, D. E. Gragson, G. L. Richmond, *Coll. Surf. A, in press* (1998) .

[17] R. A. Walker, J. C. Conboy, G. L. Richmond, *Langmuir, 13* (1997) 3070-3073.

[18] B. L. Smiley, G. L. Richmond, (submitted) .

[19] R. A. Walker, G. L. Richmond, (submitted) .

[20] C. Tanford, *The Hydrophobic Effect*, John Wiley & Sons, Inc., New York 1973.

[21] N. L. Gershfeld, *Ann. Rev. Phys. Chem., 27* (1976) 349-368.

[22] R. C. MacDonald, S. A. Simon, *Proc. Natl. Acad. Sci. USA, 84* (1987) 4089-4093.

[23] J. Mingins, J. A. G. Taylor, B. A. Pethica, C. M. Jackson, B. Y. T. Yue, *Journal of the Chemical Society, Faraday Transactions 1, 78* (1982) 323-339.

[24] J. Mingins, D. Stigter, K. A. Dill, *Biophys. J., 61* (1992) 1603-1615.

[25] H. M. McConnell, *Ann. Rev. Phys. Chem., 42* (1991) 171-195.

[26] H. Möhwald, *Ann. Rev. Phys. Chem., 41* (1990) 441-476.

[27] J. Hwang, L. K. Tamm, C. Böhm, T. S. Ramalingam, E. Betzig, M. Edidin, *Science, 270* (1995) 610-614.

[28] U. Essmann, L. Perera, M. L. Berkowitz, *Langmuir, 11* (1995) 4519-4531.

[29] S. W. Chiu, M. Clark, V. Balaji, S. Subramaniam, H. L. Scott, E. Jakobsson, *Biophys. J., 69* (1995) 1230-1245.

[30] S. J. Marrink, O. Berger, P. Tieleman, F. Jähnig, *Biophys. J., 74* (1998) 931-943.

[31] C. Hirose, N. Akamatsu, K. Domen, *Appl. Spectrosc., 46* (1992) 1051-1072.

[32] Y. R. Shen, *The Principles of Nonlinear Optics*, Wiley & Sons, Inc., New York 1984.

[33] D. E. Gragson, B. M. McCarty, G. L. Richmond, D. S. Alavi, *J. Opt. Soc. Am. B, 13* (1996) 2075-2083.

[34] J. C. Conboy, M. C. Messmer, G. L. Richmond, *J. Phys. Chem., 100* (1996) 7617-7622.

[35] A. Tadjeddine, A. Peremans, P. Guyot-Sionnest, *Surface Science, 335* (1995) 210-220.

[36] N. Bloembergen, P. S. Pershan, *Phys. Rev., 128* (1962) 606-622.

[37] B. Dick, A. Gierulski, G. Marowsky, G. A. Reider, *Applied Physics B, 38* (1985) 107-116.

[38] J. C. Conboy, J. L. Daschbach, G. L. Richmond, *J. Phys. Chem., 98* (1994) 9688-9692.

[39] R. G. Snyder, H. L. Strauss, C. A. Elliger, *J. Phys. Chem., 86* (1982) 5145-5150.

[40] R. A. MacPhail, H. L. Strauss, R. G. Snyder, C. A. Elliger, *J. Phys. Chem., 88* (1984) 334-341.

[41] C. Huang, J. T. Mason, I. W. Levin, *Biochemistry, 22* (1983) 2775-2780.

[42] D. Lin-Vien, N. B. Colthup, W. G. Fateley, J. G. Grasselli, *The Handbook of Infrared and Raman Characteristic Frequencies of Organic Molecules*, Academic Press, New York 1991.

[43] B. L. Smiley, G. L. Richmond, (in preparation) .

[44] H. Schindler, *Biochim. Biophys. Acta, 555* (1979) 316-336.

[45] D. Stigter, J. Mingins, K. A. Dill, *Biophys. J., 61* (1992) 1616-1629.

[46] D. E. Gragson, G. L. Richmond, *J. Phys. Chem. B, 102* (1998) 3847-3861.

[47] Q. Du, E. Freysz, Y. R. Shen, *Science, 264* (1994) 826-828.

[48] D. E. Gragson, B. M. McCarty, G. L. Richmond, *J. Am. Chem. Soc., 119* (1997) 6144-6152.

[49] Q. Du, R. Superfine, E. Freysz, Y. R. Shen, *Phys. Rev. Lett., 70* (1993) 2313-2316.

[50] L. F. Scatena, G. L. Richmond, (in preparation) .

[51] G. A. Jeffrey, *An Introduction to Hydrogen Bonding*, Oxford University Press, New York 1997.

[52] P. A. Gignere, *J. Raman Spec., 15* (1984) 384.

[53] J. R. Scherer, *Infrared and Raman Spectroscopy of Liquid Water, Vol. 5*, Heyden, Philadelphia 1978.

[54] A. Frenkel, M. A. Sartor, M. S. Wlodawski, *Applied Optics, 36* (1997) 5288-5297.

[55] S. Takeuchi, T. Kobayashi, *J. Appl. Phys., 75* (1994) 2757-2760.

[56] M. A. Wilson, A. J. Pohorille, *J. Am. Chem. Soc., 118* (1996) 6580-6588.

[57] R. Lingle, X. Xu, H. Zhu, S. C. Yu, J. B. Hopkins, *J. Phys. Chem., 95* (1991) 9320-9331.

Table 1:VSFS system characteristics

	System 1	System 2	System 3
pump laser	GCR-11 (Nd:YAG) (Spectra Physics)	Ti:Sapphire Regen (Coherent/Quantronix)	Infinity (Nd:YAG) (Coherent)
repetition rate	10 Hz	1 kHz	1-100 Hz
pulse duration	13 ns	2 ps	3.5 ns
ω_{vis}	532 nm	800 nm	532 nm
Energy (ω_{vis})	5 mJ	150 μJ	3 mJ
ω_{ir}	3.0 - 3.6 μm (3300 - 2800 cm^{-1})	2.7 - 4.0 μm (3700 - 2500 cm^{-1})	2.5 - 4.2 μm (4000 - 2400 cm^{-1})
Energy (ω_{ir})	1-3 mJ	2-6 μJ	1-5 mJ
ω_{ir} method	$LiNiO_3$ OPO	white light generation/OPA	OPO/OPA
ω_{ir} bandwidth	6 cm^{-1}	16-18 cm^{-1}	2 cm^{-1}
ω_{sum} window	451 - 463 nm	617 - 662 nm	439 - 472 nm
sensitivity[a]	1	10^3	10

[a]Based on Equation 3 assuming similar spot sizes for ω_{ir} and ω_{vis} and scaled to sensitivity of System 1.

Figure Captions

Figure 1. Schematic diagram of sum frequency generation at a liquid:liquid interface. To operate in a total internal reflection geometry, ω_{ir}, ω_{vis}, and ω_{sum} all pass through the medium with the higher refractive index.

Figure 2. Molecular structure of 1,2-diacyl-s*n*-glycero-3-phosphocholine.

Figure 3. Square of the Fresnel factor product governing the intensity of sum frequency response for both internal and external reflection geometries.

Figure 4. Spectra of a DLPC monolayer (55 $Å^2$/molecule) recorded under different polarization conditions. The top panel shows the spectrum recorded under PPP conditions; the middle panel depicts an SSP spectrum and the bottom panel contains an SPS spectrum. Solid lines represent fits to the data using a Voigt profile to account for the natural (Lorentzian) linewidth of the transition as well as the finite (Gaussian) bandwidth of the infrared source of System 1 (6 cm^{-1}).

Figure 5. Two limiting cases of conformational order in a monolayer composed of hydrocarbon chains. The top panel depicts an ordered monolayer in which the chains have assumed primarily all-*trans* conformations. A disordered monolayer (bottom panel) is one in which the chains contain *gauche* defects or torsional distortion along the carbon backbone.

Figure 6. Spectra of DSPC monolayers prepared by different methods. Appearing in the bottom panel is a spectrum of a DSPC monolayer at the air:water interface (55 $Å^2$/molecule) for comparison. All spectra were recorded under SSP conditions. These spectra highlight the way in which the method of monolayer preparation affects molecular ordering. Similarities between the MI monolayer (middle panel) and the monolayer at the air:water interface suggest that the multiple injection method forces the CCl_4 solvent from the acyl chain network and induces a two dimensional crystallization. The disorder within the DV

monolayer (top panel) is thought to arise from solvation of the acyl chains by the CCl_4.

Figure 7. Ordering within monolayers (r^+/d^+) of PC monomers as a function of acyl chain length (n) and monolayer preparation method. The r^+/d^+ ratios for PC monolayers at the air:water interface (55 $Å^2$/molecule) are included for comparison. Spectra of the DV, MI, and SS monolayers were recorded using System 1. Spectra of monolayers at the air:water interface were acquired using System 2. To within experimental error, the calculated ratios are unaffected by the bandwidth difference between the two laser systems.

Figure 8. Spectrum of equilibrated DLPC monolayer showing both CH and OH stretching regions. This spectrum was recorded with System 2 under SSP conditions. Intensity above 3000 cm^{-1} is due to vibrational motion of the aqueous solvent molecules.

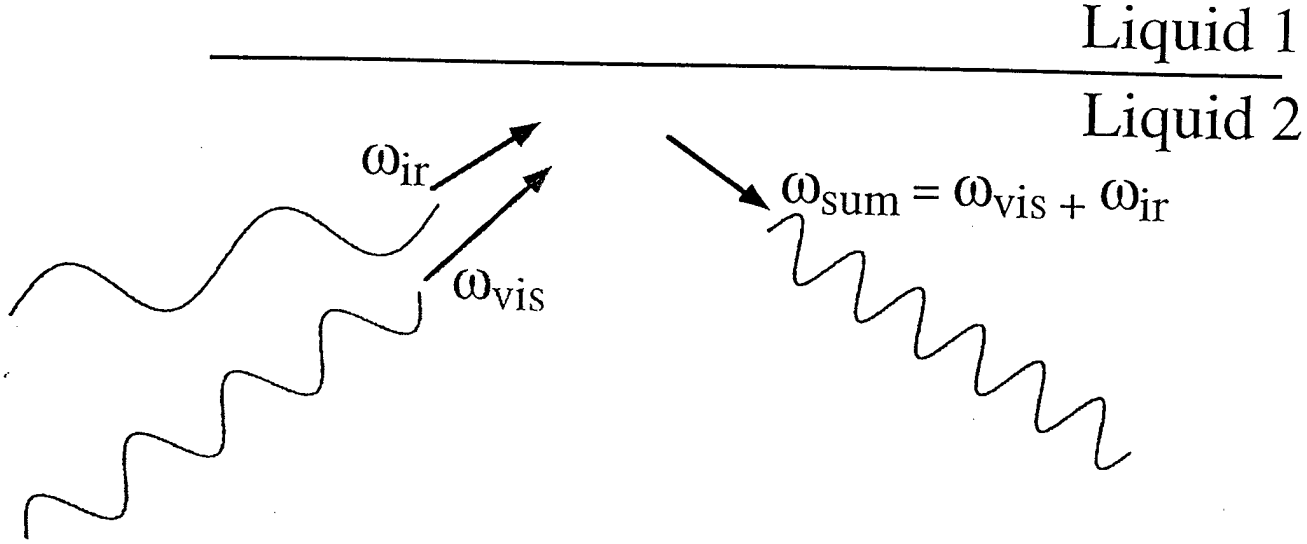

Spectroscopy

Figure 1

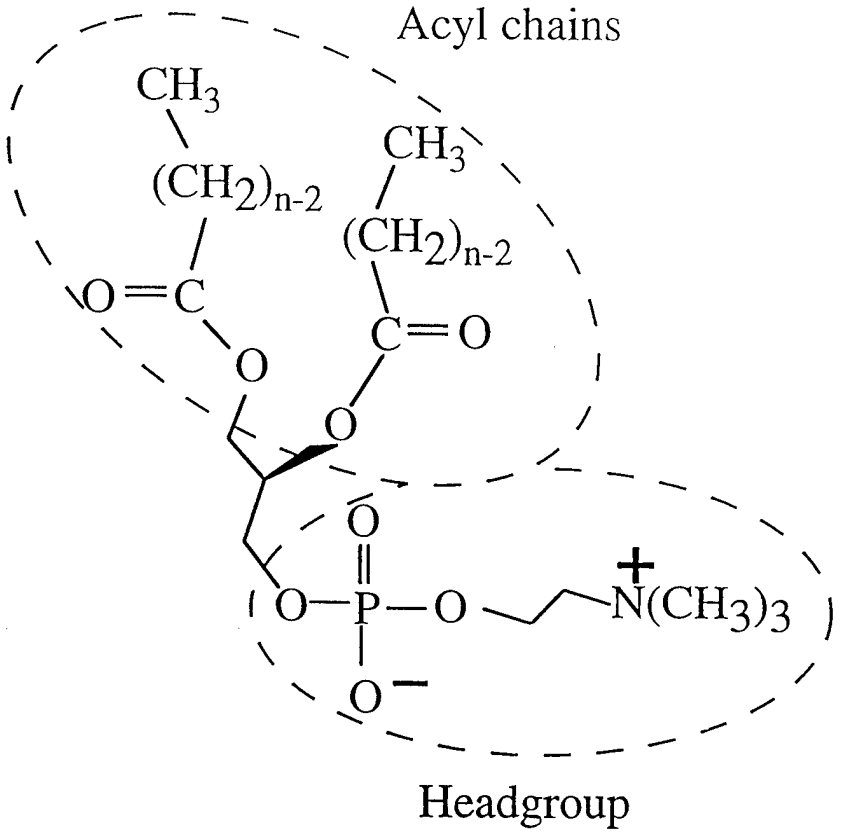

Spectroscopy

Figure 2

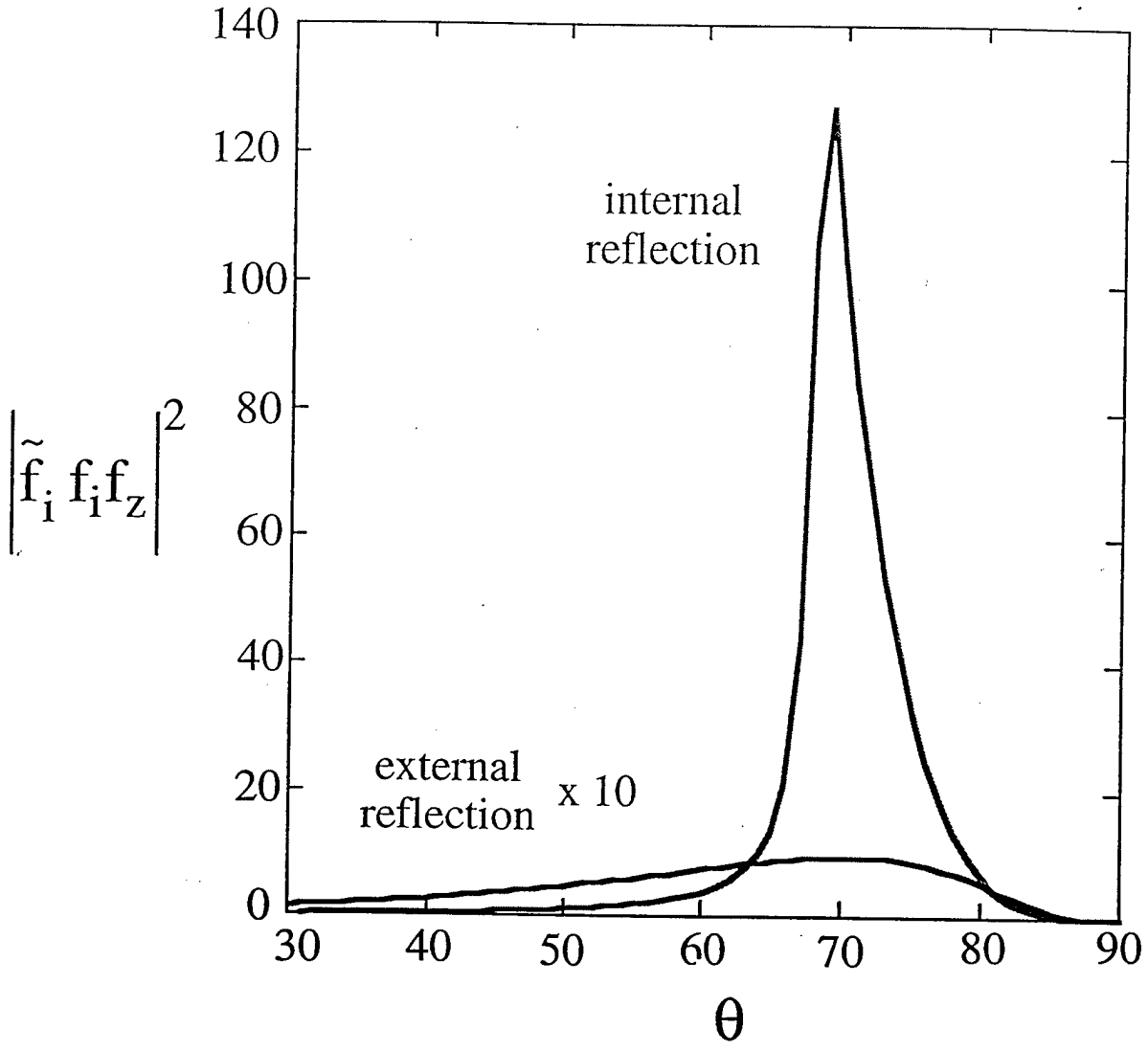

Figure 3

Spectroscopy

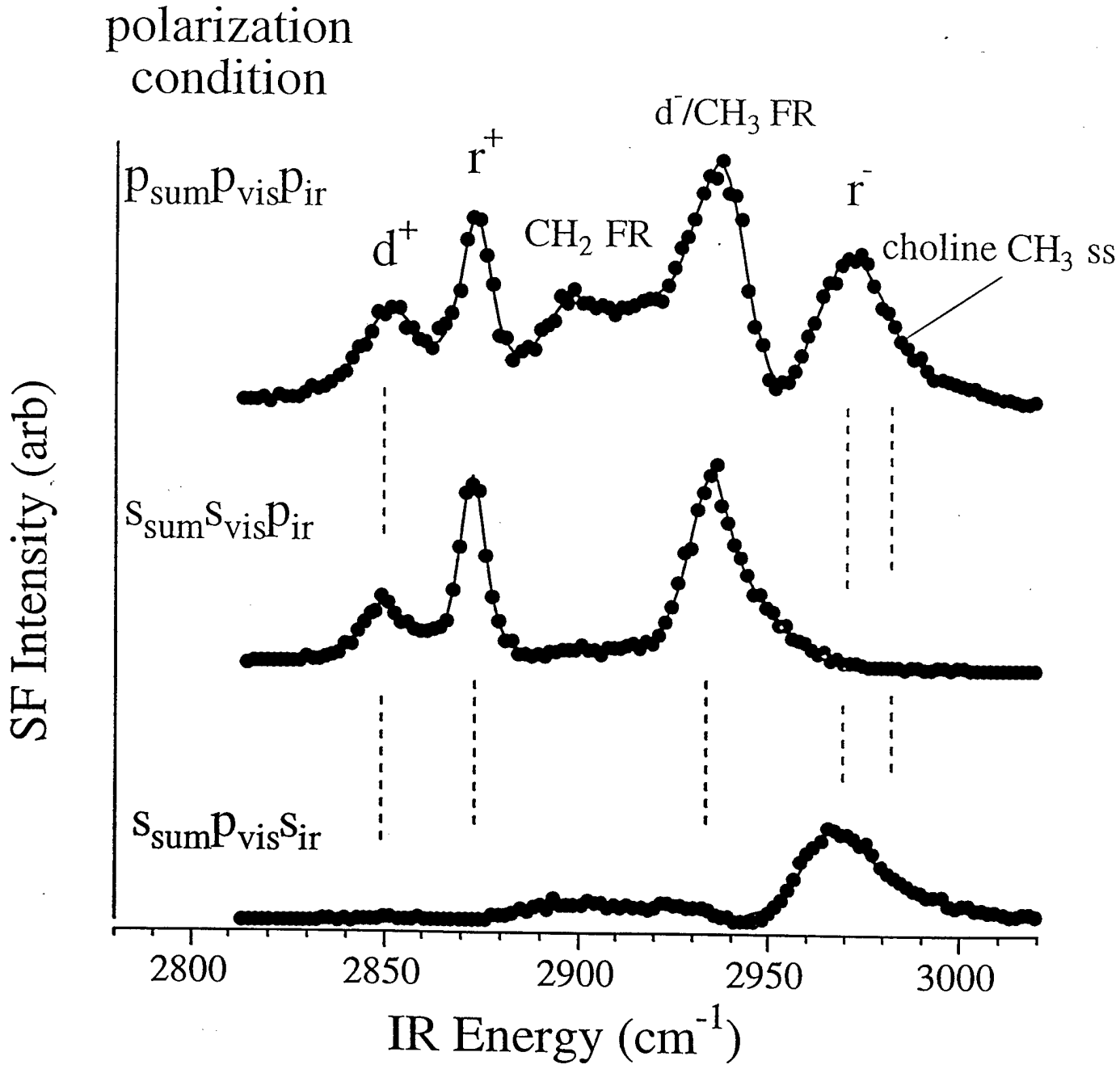

Spectroscopy

Figure 4

Ordered

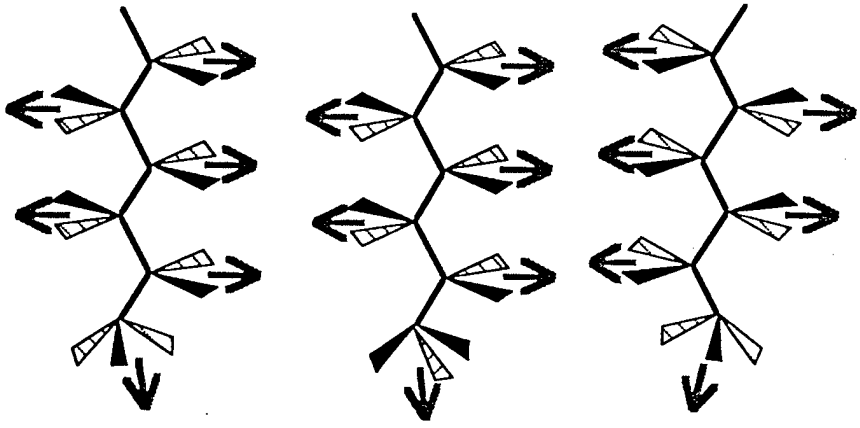

Disordered

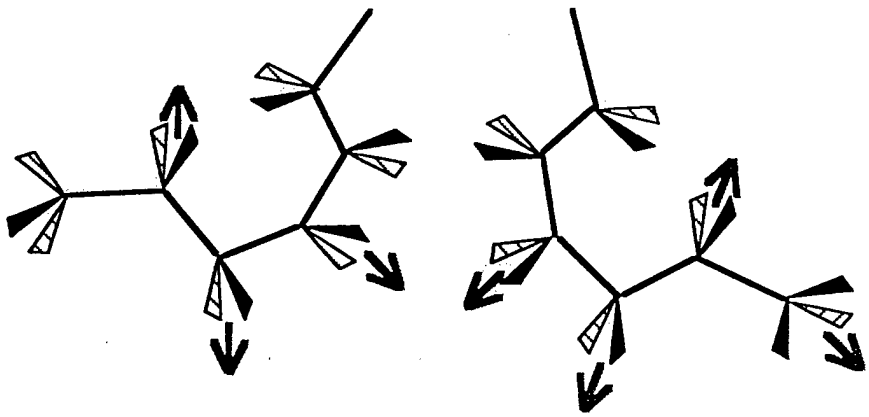

Spectroscopy

Figure 5

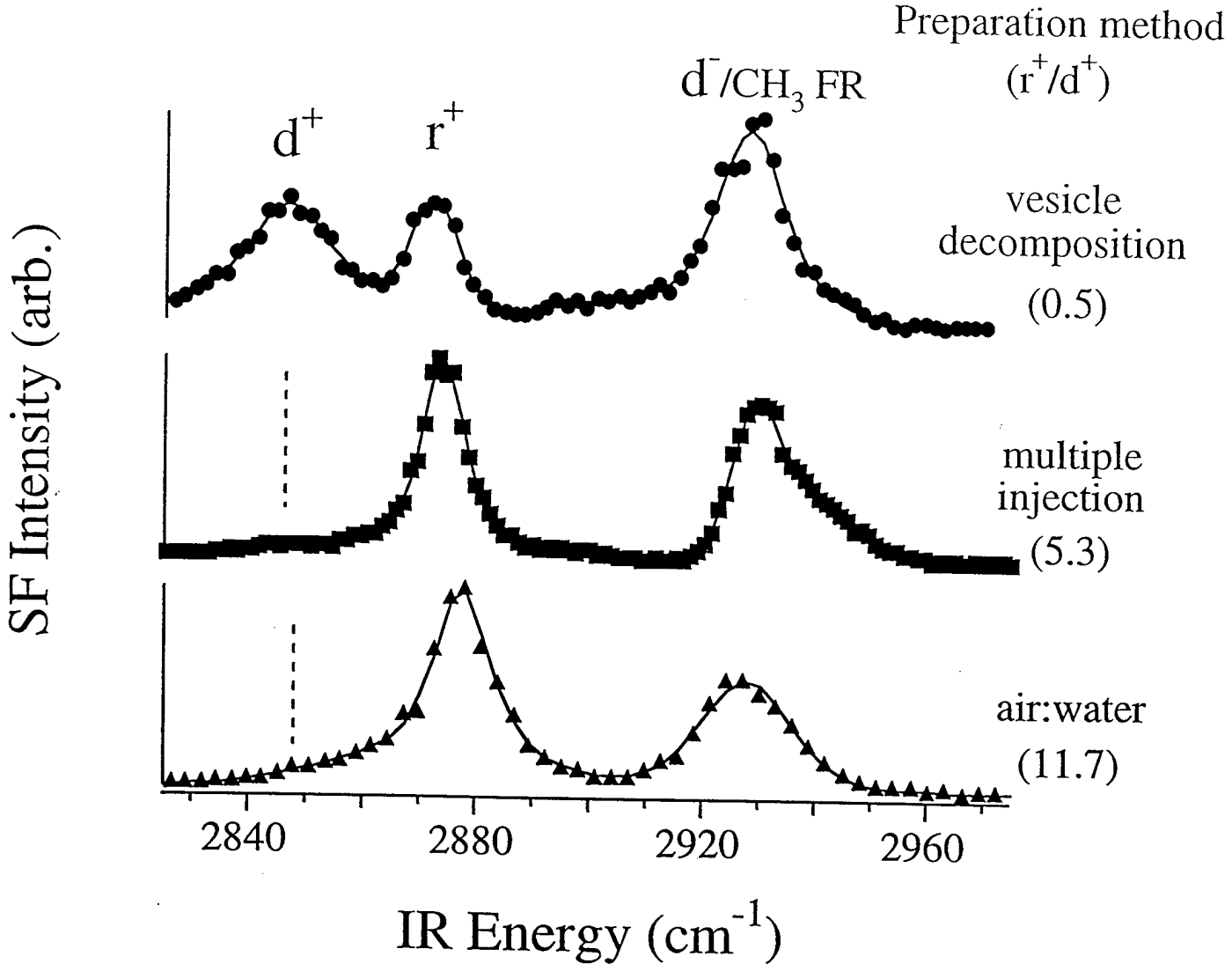

Spectroscopy

Figure 6

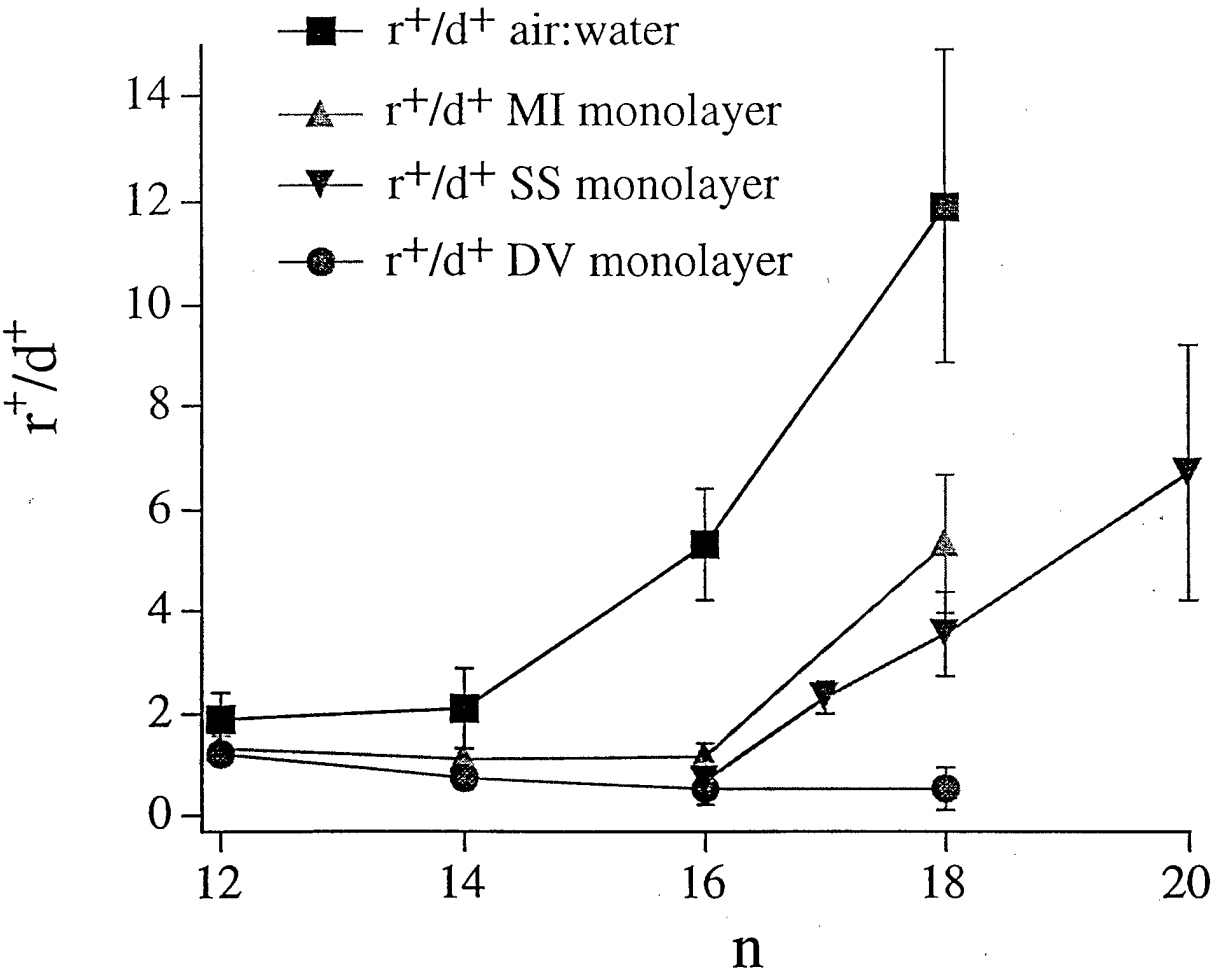

Spectroscopy

Figure 7

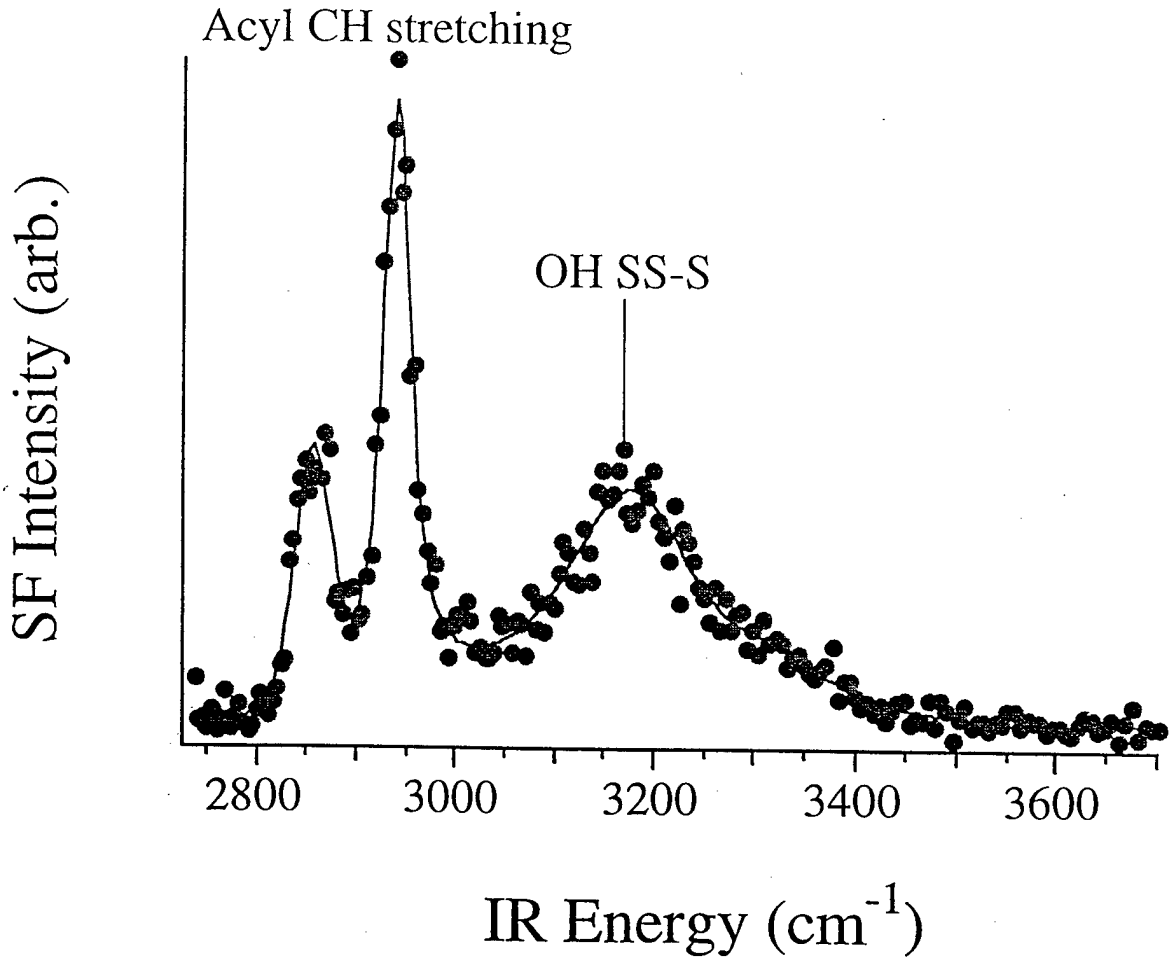

Spectroscopy

Figure 8